The Habitable-zone Planet Finder: A status update on the development of a stabilized fiber-fed near-infrared spectrograph for the for the Hobby-Eberly telescope

Mahadevan, Suvrath, Ramsey, Lawrence, Terrien, Ryan, Halverson, Samuel, Roy, Arpita, et al.

Suvrath Mahadevan, Lawrence W. Ramsey, Ryan Terrien, Samuel Halverson, Arpita Roy, Fred Hearty, Eric Levi, Gudmundur Kari Stefansson, Paul Robertson, Chad Bender, Chris Schwab, Matt Nelson, "The Habitable-zone Planet Finder: A status update on the development of a stabilized fiber-fed near-infrared spectrograph for the for the Hobby-Eberly telescope," Proc. SPIE 9147, Ground-based and Airborne Instrumentation for Astronomy V, 91471G (24 July 2014); doi: 10.1117/12.2056417

SPIE.

Event: SPIE Astronomical Telescopes + Instrumentation, 2014, Montréal, Quebec, Canada

The Habitable-zone Planet Finder: A status update on the development of a stabilized fiber-fed near-infrared spectrograph for the Hobby-Eberly telescope

Suvrath Mahadevan[a,b], Lawrence W. Ramsey[a,b], Ryan Terrien[a,b], Sam Halverson[a,b], Arpita Roy[a,b], Fred Hearty[a], Eric Levi[a], Gudmundur Kari Stefansson[a,b], Paul Robertson[a], Chad Bender[a], Chris Schwab[a], Matt Nelson[c]

[a]Department of Astronomy & Astrophysics, The Pennsylvania State University, 525 Davey Laboratory, University Park, 16802, USA.
[b]Center for Exoplanets & Habitable Worlds, The Pennsylvania State University, University Park, PA 16802.
[c]Department of Astronomy, University of Virginia, P.O. Box 400325, Charlottesville, VA 22904-4325, USA;

ABSTRACT

The Habitable-Zone Planet Finder is a stabilized, fiber-fed, NIR spectrograph being built for the 10m Hobby-Eberly telescope (HET) that will be capable of discovering low mass planets around M dwarfs. The optical design of the HPF is a white pupil spectrograph layout in a vacuum cryostat cooled to 180 K. The spectrograph uses gold-coated mirrors, a mosaic echelle grating, and a single Teledyne Hawaii-2RG (H2RG) NIR detector with a 1.7-micron cutoff covering parts of the information rich z, Y and J NIR bands at a spectral resolution of R$\sim$50,000. The unique design of the HET requires attention to both near and far-field fiber scrambling, which we accomplish with double scramblers and octagonal fibers. In this paper we discuss and summarize the main requirements and challenges of precision RV measurements in the NIR with HPF and how we are overcoming these issues with technology, hardware and algorithm developments to achieve high RV precision and address stellar activity.

Keywords: Exoplanets, spectroscopy, near-infrared spectrograph design, instrumentation, modal noise, fibers, scrambling

1. INTRODUCTION

The Habitable-Zone Planet Finder (HPF)[1] is a stabilized near-infrared (NIR) fiber-fed high-resolution (R$\sim$50,000) spectrograph being built at Penn State as a facility-class instrument for the 10m Hobby-Eberly Telescope (HET) in Texas. Its main scientific goal is to search detect and confirm low mass planets in the Habitable Zones of mid-late type M dwarfs using the Doppler radial velocity technique. The fiber-fed HPF incorporates many lessons learnt from optical precision radial velocity spectrographs like HARPS and PARAS[2] as well our experience with the Penn State Pathfinder NIR prototype[3] and the SDSS-III APOGEE spectrograph.[4] Significant challenges of working at these new wavelengths are being overcome with ongoing research and technology development, with HPF slated to be commissioned at the HET in 2016.

The scientific motivations for a NIR RV instrument have been discussed before, and the importance and advantages of surveying M dwarfs for planets has also been discussed in numerous recent refereed papers. The importance of M dwarfs will only increase as new surveys like K2 & TESS find more planets around them. Our goal in this overview paper is to present a status update on the HPF project and discuss specific subsystems and ongoing R&D in more detail. We point the interested reader to other papers from the HPF team in these proceedings that focus on environmental control (*Hearty et al.*), fiber feed (*Roy et al.*), calibration system (*Halverson et al.*), simulations of RV performance (*Terrien et al.*) and the detector subsystem (*Bender et al.*)

E-mail: suvrath@astro.psu.edu, Telephone: 1 814 865 0261

Ground-based and Airborne Instrumentation for Astronomy V, edited by Suzanne K. Ramsay, Ian S. McLean, Hideki Takami, Proc. of SPIE Vol. 9147, 91471G · © 2014 SPIE · CCC code: 0277-786X/14/$18 · doi: 10.1117/12.2056417

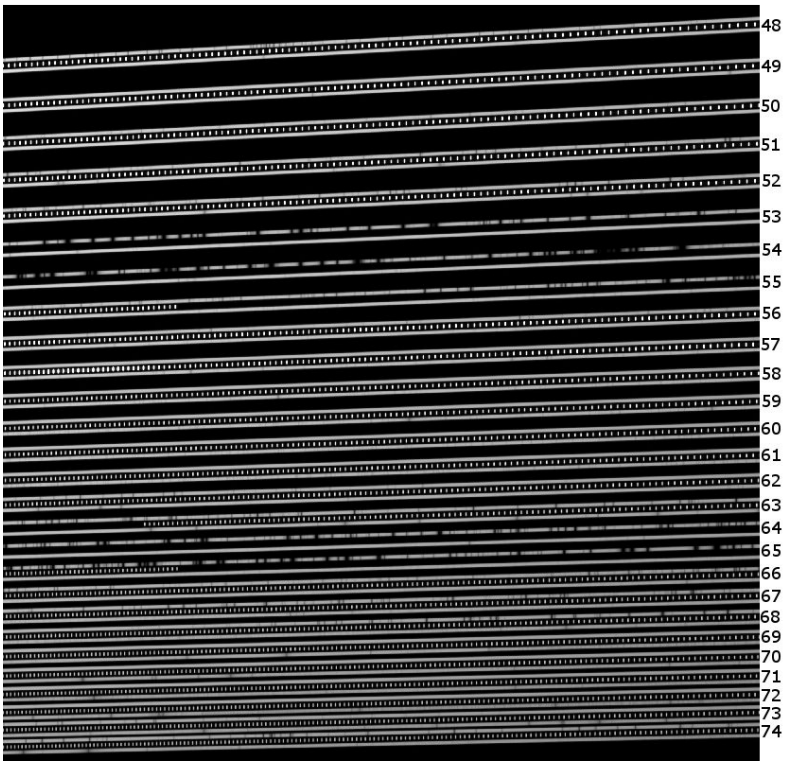

Figure 1. Spectral format and order coverage for HPF. Three fibers are shown, corresponding to sky, science and frequency stabilized laser comb light.

2. SPECTRAL FORMAT

HPF is designed to observe part of the RV-information rich (for M dwarfs) parts of the z,Y and J bands at a resolution of R∼50,000 on a single Hawaii-2RG NIR array. The use of a single array yields almost complete order coverage at the blue wavelengths (z), but only partial order coverage at the reddest wavelengths (J). Figure 1 shows the spectral format and order numbers of the HPF fibers. Fibers corresponding to science, calibration, and sky are shown. The science fiber shows telluric absorption. The calibration fiber shows the laser comb light. The use of three separate filter cavities leads to incomplete wavelength coverage for comb light, but the gaps correspond to gaps between the Z, Y and J bands where the large number of water vapour lines limits the use for precision RV applications.

3. SPECTROGRAPH OPTICS

We have explored various design options that meet the top-level science requirements. The baseline approach we chave chosen to adopt is the well-proven quasi-Littrow white pupil design with a monolithic off-axis parabolic collimator, a 200 mm by 800 mm 31.6 g/mm replicated mosaic grating from Newport Richardson Gratings Lab (RGL) blazed at 74.6 degrees (as manufactured), a VPH cross disperser, and a fast refractive camera made with standard Schott and Ohara glasses. The white pupil enables good control of the scattered light and minimizes the size of the cross-disperser and camera apertures. The use of an asymmetric white pupil design enables higher groove density on the VPH and is the design adopted for HPF. The large mosaic echelle grating has been used in UVES and HARPS, and is a standard product from Newport RGL. and is now in hand. Input optics made from CaF2 and SFTM-16 reimage the input fiber feed from f/3.3 (accounting for FRD from the telescope input of f/3.65) to the f/8 that the off-axis parabola is expecting. The grating and all mirror are designed on Zerodur substrates. Details of the spectrograph optical design merits its own paper, which we intend to publish along with final refractive indices and melt data. We do note that the large $A\Omega$ of the HET (ie. 10m telescope with

1.5 arcsecond median seeing) leads to a challenging design for HPF compared to existing optical precision RV spectrographs due to large field curvatures and the fast camera required. All of the spectrograph optics are mounted on an 8 foot long Al-60661-T6 bench. The temperature of the bench and optics is controlled to within a few milli-kelvin of 180K.

4. THE HPF DETECTOR SYSTEM AND H2RG 1.7 MICRON CUTOFF DETECTOR

The HPF detector subsystem will use a Hawaii-2RG (H2RG) 1.7μm cutoff HgCdTe device with 2048x2048 pixels, connected to a SIDECAR application specific integrated circuit (ASIC). These devices are operated through a SIDECAR Acquisition Module (SAM) controller board. We purchased two H2RG devices, one engineering grade and one science grade, a SIDECAR, and a SAM from Teledyne Imaging Systems (TIS), and took delivery in 2013. We opted to use a 1.7μm cutoff device after carrying out a trade study which compared the expected thermal background and operating temperatures from the 1.7μm and 2.5μm configurations. The 1.7μm devices have slightly lower quantum efficiency (QE) and have been more difficult for TIS to manufacture. However, our trade study indicated that using a 1.7μ device would allow us to operate the HPF cryostat at $\sim$180 K, while supressing the contribution of thermal background to less than the dark current. Conversly, a 2.5μ device would require an operating temperature of $\sim$135 K or lower, or would require the use of thermal blocking glasses such as PK-50 to suppress the Urbach tail[5] which stretches out past 3μm, to achieve comparable thermal suppression. We deemed the benefits of a warmer operating temperature and camera design without blocking glass provided by a 1.7μ device to outweigh the quantum efficiency and manufacturing risks. The science and engineering grade detectors we received were characterized by TIS: the science grade device has QE ranging from $\sim$65 – 80% over the wavelength range of 0.8 – 1.5μm, while the engineering grade ranges from $\sim$50 – 60%. Both have low read-noise (CDS <20 electrons) and low dark current (<0.02 electrons/s), with the science grade array expected to exhibit very low persistence.

We are currently carrying out laboratory testing and characterization of our H2RGs, ASIC, and SAM to acquire operating proficiency and develop the detetctor control software for HPF. We are using a GL Scientific (GLS) SSC-g2 Stirling Cooler Cryostat system to facilitate these tests. To date, our efforts have concentrated exclusively on our engineering device; we expect to begin work on the science device in Fall 2014. We cool the H2RG and ASIC subsystem with a Sunpower Stirling cooler, which provides a 65 K coldfinger attached to the GLS molybdenum mounting package. We actively maintain the detector temperature at 120 K with a Lakeshore 336 temperature controller. This subsystem is surrounded by an inner sanctum radiation shield, inside the GLS vacuum vessel, which operates at a temperature of $\sim$100 K; this temperature is stable, but not actively controlled.

When integrated into HPF, the H2RG and ASIC will be mounted into the inner sanctum subcomponent of the SSC-g2. The cooling power for this system will be provided by a Cu strap to the HPF LN2 tank, and the temperature actively controlled by a Lakeshore 336 temperature controller.

Our laboratory testing has included the fundamental, but critical, steps of optimizing the SIDECAR bias voltages to minimize detector noise while providing stable readout and desired well depth. We use the GLS system with a cold plate covering the inner sanctum to measure the read-noise of our engineering grade H2RG, and to characterize the gain of each SIDECAR amplifier. This H2RG device has a photo-emissive spot which generates sufficient scattered light inside the GLS system to prevent us from fully characterizing the dark current. We also use the GLS system with a thermal blocking filter in place of the inner sanctum cold plate to characterize the detector linearity and well depth, charge persistence, and interpixel capacitance. Results from each of these tests are described further in *Bender et al.* in these proceedings.

5. CRYOSTAT, RADIATION SHIELD, AND ENVIRONMENTAL CONTROL

The HPF spectrograph must be kept cold to prevent saturation of the NIR detector by ambient radiation at room temperature. The choice of the H2RG 1.7μm detector enables HPF to work at a temperature of 180 K. The precision RV requirements also necessitate a high level of temperature control to prevent mechanical drifts, thermal contraction and expansion, and refractive index changes from adversely impacting the RV precision. The design of the cryostat and environmental control system are described in more detail by *Hearty et al.*(these

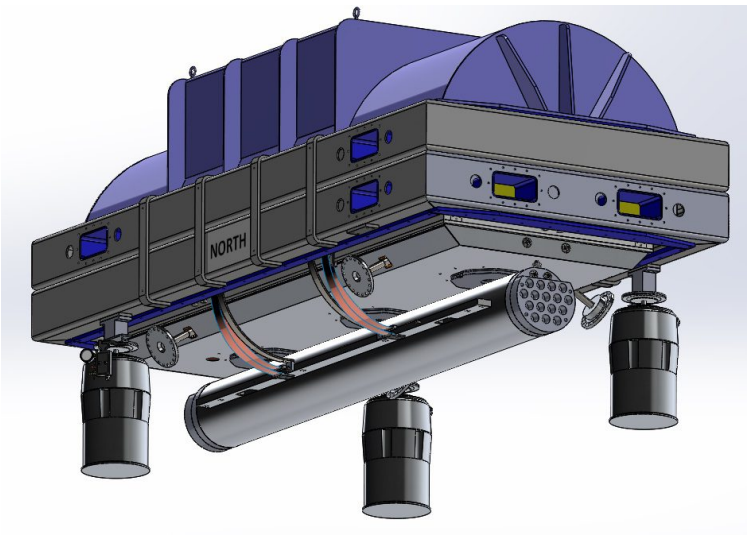

Figure 2. The HPF cryostat shell that maintains the vaccum and houses radiation shield, bench, and optics. Bottom half of the cryostat is hidden to more clearly show the LN2 cylinder, charcoal getters attached to the cylinder and trantorques that penetrate throught the radiaition shield and restrain the bench during shipping.

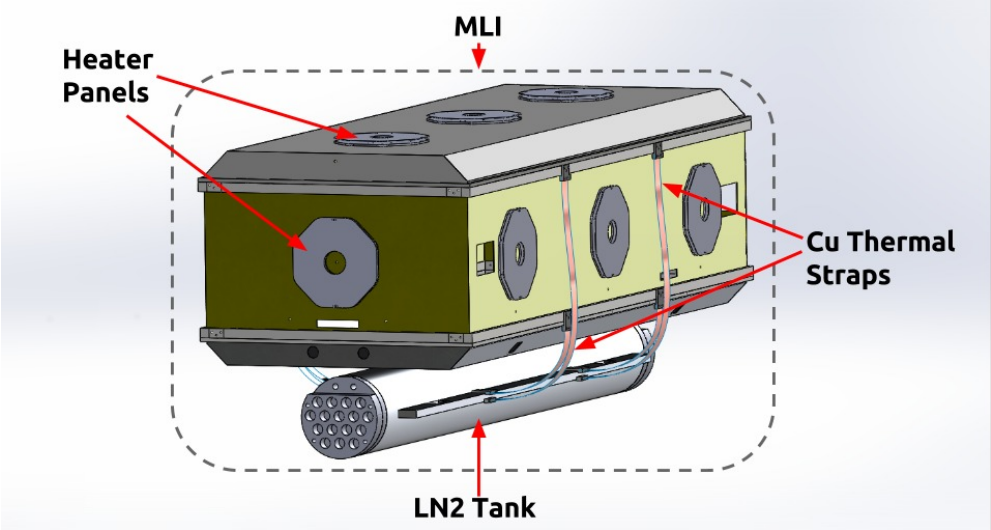

Figure 3. The radiation shield - a vacuum chamber which contains the instrument optics - along with the LN2 tank is covered in MLI blankets for thermal insulation, and along with the copper thermal straps and the heater panels, they are responsible for keeping the HPF at 180K at milli-Kelvin precision.

proceedings). Scale model tests described in that paper verify our design and the ability to control the environment of the cryostat at a level approaching 1 milli-Kelvin. Figure 2 shows the outer vaccum vessel being manufactured by Pulseray and Figure 3 shows the radiation shield, liquid nitrogen tank, the heater panels, a subset of the copper straps and the MLI blankets that together make up the physical components of the active environmental control system for HPF. Salient elements of the overall design are discussed here

Vacuum: The HPF thermal control system is designed to operate in a high vacuum environment. At pressures of 10^{-6} torr or lower convection is negligible and only the effect of radiation and conductive paths have to be addressed. Our thermal and environmental control is build around the existence of this high vacuum enabled by the charcoal getters attached to the liquid nitrogen tanks that aid in maintaining the high vacuum. We note that instruments working at significantly lower vacuum will have to account for thermal effects from

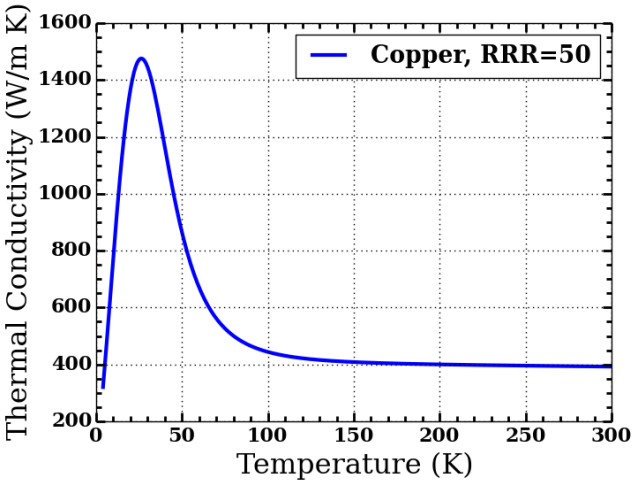

Figure 4. The thermal conductivity of copper as a function of temperature from the NIST cryogenics website. We see a non-negligible change in thermal conductivity in the 77K to 180K range. We are assuming a Residual-Resistance Ratio (RRR) of 50 for our copper straps.

convection or molecular transport as well if they wish to adapt our environmental control system.

Liquid Nitrogen: The liquid nitrogen provides the passive cooling for the instrument. To prevent variations in the temperature of the LN2 due to atmospheric pressure changes the pressure in the LN2 is maintained at a slight positive pressure (compared to the atmospheric pressure) with a backpressure regulator. The radiation shield (and instrument within) is cooled by connecting the shield to the LN2 tank with 16 copper thermal straps. The LN2 talk is suspended from the cryostat walls instead of the bench to prevent its changing weight (as LN2 boils off) from affecting the instrument RV precision.

Copper Straps: The straps need to be sized properly to cool the shield down to temperatures slightly cooler (around 160K - 170K) than the 180K-end temperature goal. The heater panels are used to warm up the radiation shield and actively control the temperature at 180K. To calculate the size of the copper straps correctly it is necessary to account for the temperature dependant thermal conductivity (k) of copper (Figure 4) and calculate the heat flow we integrate over the entire range

$$H_{Cu} = \frac{dQ}{dt} = \frac{A}{L}\int_{T_C}^{T_H} k(T)dT, \tag{1}$$

where H_{Cu} is the heat flow, k is the thermal conductivity of copper, $T_C = 77K$ is the LN2 temperature, and $T_H = 160 - 170K$ is the desired temperature of the radiation shield before active heating, and L and A are the length and cross-sectional area of our thermal strap, respectively. Using the correct thermal conductivity as a function of wavelength allows us to correctly calculate the length of the copper straps to bright the radiation shield to the desired temperature.

Heating Panels: The Cu thermal straps will be sized to cool the spectrograph to 170K, and the target temperature of 180K will be maintained with a set of electrical heater panels controlled by a closed-loop software system. The body of the thermal enclosure will be covered with 14 regular octagonal aluminum heater panels (3 per side, plus one on each face), each having a side length of 5 inches. Within each heater panel is an arrangement of 4 Vishay Dale RH005 5W/150Ω chassis-mount resistors (Figure 5), which provide the electrical heating. The resistors are wired such that the total circuit resistance of a single panel is 150Ω. While we are currently controlling the ECS with a custom microcontroller and software system, the 150Ω per channel resistance allows for compatibility with a Model 336 temperature controller from LakeShore Cryotronics. Individual Vishay resistors are also placed on each of the bench hangers for additional control. Temperature sensors placed on

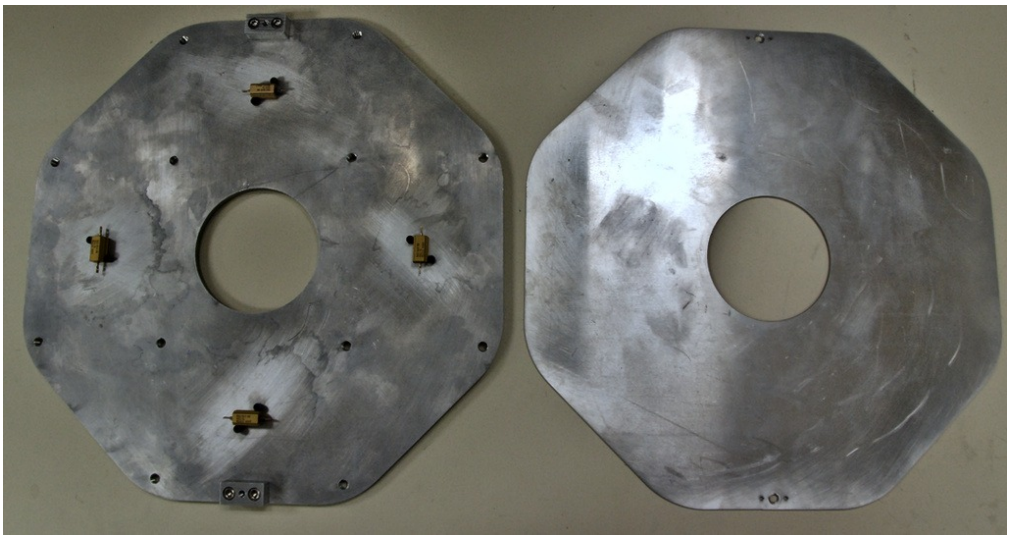

Figure 5. Aluminium panel heater with Vishay resistive heaters and protective cover. The Vishay heaters are mounted to the panel using indium foil to enhance thermal contact.

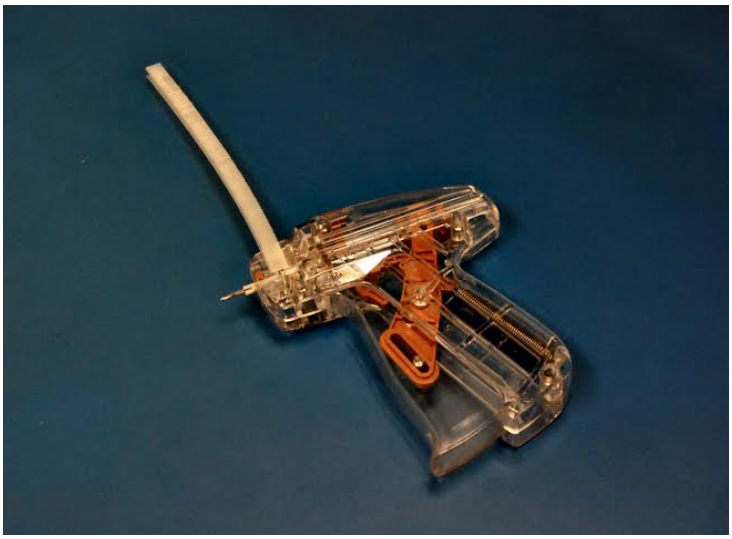

Figure 6. A tag gun and nylon I-pins being used to build MLI blankets. The tag guns we use are TagStar XB tag guns with 3.5mm and 5 mm I pins purchased from Jaygroups in Bangalore, India.

the inside of the radiation shield in close proximity to the heaters will control the heat output to achieve high temperature stability. Two sets of redundant temperature sensors are baselined for the heater panels: a constant current drive of a forward biased diode, and a commercial calibrated CERNOX sensor from Lakeshore. The ECS heater system is carefully wired to ensure modularity and preservation of the vacuum environment. The heaters are wired with LakeShore WHD-30 cryogenic wire, which is insulated with Teflon to prevent outgassing. The three heater panels along each side of the thermal enclosure connect to a wire harness, with the two face panels comprising a fifth harness. Each panel has an individual connector to its wire harness to facilitate quick replacement in the event of a failure. The wire harnesses are collected into 32-pin hermetic connectors at the vacuum interface, where they are then connected to the microcontroller.

MLI Blanket: The MLI blankets that cover the radiation shield are made of 12-24 layers of Mylar, layers separated from each other by a nylon mesh layer to prevent conductive paths. 3.5mm and 5mm I shaped nylon tag

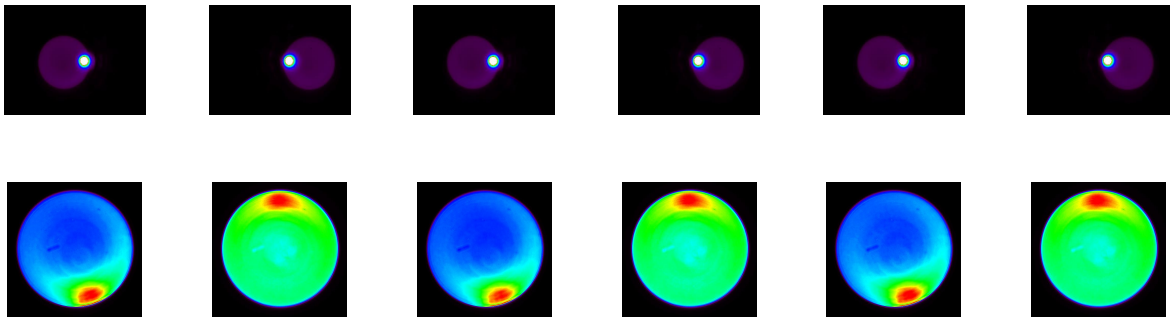

Figure 7. Input into a 300 μm circular fiber (top) and near field output (bottom) from the fiber. The variability of illumination is clearly seen.

pins inserted with a tag gun (both pins and tag guns are commercially available from the garment industry, ours purchased from jaysgroups.com) are used to hold the blanket layers in place in combination with limited stitching at the seams and edges. The main purpose of the MLI blanket is to significantly decrease the radiative heat load of on the instrument. While the exact performance of MLI blanket is highly dependent on manufacturing, we expect to be able to achieve an emissivity of $e_{\rm eff} \sim 0.01$ or better based on experience with SDSS-III APOGEE.[4] The sizing of the copper straps can be adjusted (within limits) to accommodate the performance of the as-built MLI blanket.

6. FIBERS, SCRAMBLING, CALIBRATION & MODAL NOISE MITIGATION

The Wide Field Upgrade (WFU) to the Hobby-Eberly telescope, being implemented for the Hobby Eberly Telescope Dark Energy Experiment (HETDEX), sets the image scale, and mounting scheme for the HPF fibers, which are effectively located at the prime focus of the telescope with no additional optics to change the focal ratio. The HPF fibers are therefore fed at the F-number of the HET itself $\sim f/3.65$. A 40m-fiber run will drop down from the prime focus and route through the telescope bearing to the basement spectrograph room. Details of the fiber feed are provided in a paper by *Roy et al.* in these proceedings. We discuss some salient points:

Choice of Fiber Type & Size: We have converged on Polymicro FBP or FIP fibers as offering the best combination of efficiency and FRD for the wavelength range of HPF, and 300 μm diameter fibers as the choice for HPF. Both circular and octagonal fibers are available at this core size. The plate scale at the HET prime focus is 177μm/arcsec. A Gaussian seeing disk with FWHM 1.5" translates to a physical extent of 265.5μm at EE50. While the upgrade will improve HET image quality, we assume a conservative seeing of 1.5", which motivates the choice of the 300 μm fiber.

Differential Atmospheric Refraction: The combination of the design of the HET, limiting it to a narrow range in sec(z) and the long wavelength operating range of HPF (which are less susceptible to atmospheric refraction) means that an Atmospheric Dispersion Corrector (ADC) is *not required* for HPF. While a significant amount of change in not expected within the HPF band pass, we emphasize that guiding in the I or Z bands (as opposed to V or R) is necessary to ensure that the star remains within 0.1" of the fiber center on average.

Scrambling: The fixed elevation and roving pupil design of the HET leads to changes in the illumination profile across a track. This, and more traditional guiding errors necessitate a high level of scrambling gain in the fiber train to enable the input variations to be largely decoupled from the output. Figure 7 shows the large variation in near field output when the input to a circular fiber is changed. This would manifest as changes in the radial velocity that could not be easily calibrated. Recent R&D work at Penn State has demonstrated very high scrambling gain with a new double scrambler design and the use of Octagonal fibers. Figure 8 shows the same test with two octagonal fibers coupled with a double scrambler. These are described in more detail in *Roy et al.* in these proceedings.

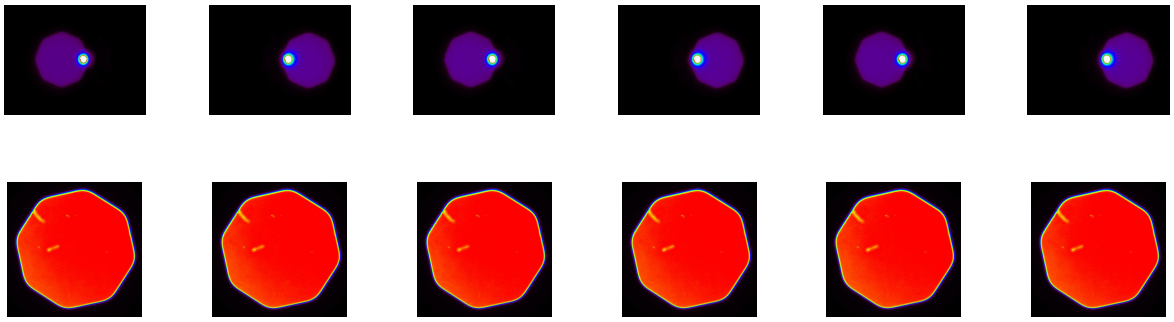

Figure 8. Input into a 300 μm octagonal fiber (top) and near field output (bottom) from s second octagonal fiber coupled to the first one with a double scrambler. No output illumination changes are discernable as the input illumination varies.

Modal Noise: The finite number of modes travelling in the fiber leads to modal noise, which is exacerbated in the NIR due to the longer wavelength (ie. smaller number of modes). We have successfully demonstrated the mitigation of modal noise for bright calibration sources using a moving holographic diffuser and an integrating sphere yielding modal scrambling both spatially and temporally.[6] In these proceedings *Halverson et al.* improve on this method by using a rotating mirror inside an integrating sphere as part of the design of the HPF calibration system.

7. CALIBRATION

Like every precision RV spectrograph HPF needs calibrators to simultaneously monitor instrument drift. In our case the following primary calibrators are being envisioned. **Laser Frequency Comb:** An ongoing collaboration between the HPF team and NIST in now developing a laser comb system to operate at the HET and be part of routine survey operation for HPF. This system provides the absolute frequency reference for all HPF calibrations. **Fiber Fabry Perot:** Ongoing R&D at Penn State developed single mode fiber fabry perot devices that offer many advantages in stability, rugged design, and lack on sensitivity to illumination or vibration. Initial tests with a commercial version are have already been published[7] and new etalons are being fabricated and tested at Penn State and NIST. Short-term stability of better than 1 m/s looks well within reach to complement the comb **Uranium-Neon Hollow Cathode Lamps:** We have demonstrated the utility of uranium neon (U/Ne) hollow-cathode lamps in the NIR, and have published derived line-lists using a Fourier Transform Spectrograph (FTS),[8] as well as a spectroscopic atlas calibrated with a laser frequency comb.[9] U/Ne hollow-cathode lamps are commercially available from Photron, and are available for HPF. Our calculation show however that due to wide variability in flux between the U and Ar lines, achieving 1m/s will be hard with these lamps alone. They are available for long term monitoring and traceability while the photonic sources are used daily and for the bulk of the precision RV work.

8. STELLAR ACTIVITY

To actually approach or achive a goal RV precision of 1 m s^{-1} in the NIR, it will be essential to not just consider hardware and alogrithmic issues, but also to mitigate the effects of Doppler contributions from stellar activity. For M stars, stellar activity may create RV signals or noise via the short-timescale convective motions known as granulation,[10] flares,[11] or magnetic activity.[12] For the most part, observations compromised by flares may be discarded, and granulation effects will largely average out over our exposure times (15-30 min). On the other hand, magnetic activity (typically in the form of starspots and long-period activity cycles) may either hide or imitate exoplanet signals,[13,14] and must be carefully scrutinized in any highly precise RV survey.

The importance of correctly treating activity-induced RV to the mission of HPF–discovering low-mass planets in the habitable zones of M stars–is illustrated by our recent work on the multi-planet system Gliese 581.[14] Rotating starspots and/or active regions induce (semi-)periodic RV signals at the rotation period and its harmonics

($P/2$, $P/3$...)[15] For many of the old, slowly-rotating M stars HPF will target, harmonics of the rotation period fall in the same period range occupied by planets in the habitable zone. In the case of GJ 581, the rotation period is 130 days, and rotating active regions create RV aliases at 66 ($P/2$) and 33 ($P/4$) days. These aliases were previously ascribed to the potentially habitable zone "planets" d[16,17] and g,[18] respectively. Fortunately, our analysis and correction of the activity (via the Hα line) suggests such insidious effects may be correctable; in addition to eliminating the signals of the false positive candidate planets, our activity correction significantly boosted the statistical significance of the real super-Earth planets c and e in the system.

We intend to continue developing our stellar activity analysis treatment in parallel with the development and commissioning of HPF. Although wavelength-dependent RV measurements of the Sun via the F/F′ technique suggest stellar velocity noise should be significantly reduced in the NIR,[19] it is still necessary to verify that any Doppler signals recovered by HPF are in fact planetary. In addition to refining our activity correction algorithm, once HPF comes online we will work to identify and characterize suitable NIR spectral activity tracers. Previous analyses of the NIR calcium II triplet ($\lambda\lambda 8498, 8542, 8662$ Å)[20] and sodium I doublet($\lambda\lambda 8183, 8194$ Å)[21,22] suggest these lines are promising candidates, but we intend to investigate other lines as well.

ACKNOWLEDGMENTS

This work was partially supported by funding from the Center for Exoplanets and Habitable Worlds. The Center for Exoplanets and Habitable Worlds is supported by the Pennsylvania State University, and the Eberly College of Science. We acknowledge support from NSF grants AST 1006676, AST 1126413, AST 1310885, and the NASA Astrobiology Institute (NNA09DA76A) in our pursuit of precision radial velocities in the NIR.

REFERENCES

[1] Mahadevan, S., Ramsey, L., Bender, C., Terrien, R., Wright, J. T., Halverson, S., Hearty, F., Nelson, M., Burton, A., Redman, S., Osterman, S., Diddams, S., Kasting, J., Endl, M., and Deshpande, R., "The habitable-zone planet finder: a stabilized fiber-fed NIR spectrograph for the Hobby-Eberly Telescope," in [*Society of Photo-Optical Instrumentation Engineers (SPIE) Conference Series*], *Society of Photo-Optical Instrumentation Engineers (SPIE) Conference Series* **8446** (Sept. 2012).

[2] Chakraborty, A., Mahadevan, S., Roy, A., Dixit, V., Harvey Richardson, E., Dongre, V., Pathan, F. M., Chaturvedi, P., Shah, V., Ubale, G. P., and Anandarao, B. G., "The PRL Stabilized High-Resolution Echelle Fiber-fed Spectrograph: Instrument Description and First Radial Velocity Results," *Publication of the Astronomical Society of the Pacific* **126**, 133–147 (Feb. 2014).

[3] Ycas, G. G., Quinlan, F., Diddams, S. A., Osterman, S., Mahadevan, S., Redman, S., Terrien, R., Ramsey, L., Bender, C. F., Botzer, B., and Sigurdsson, S., "Demonstration of on-sky calibration of astronomical spectra using a 25 GHz near-IR laser frequency comb," *Optics Express* **20**, 6631 (Mar. 2012).

[4] Wilson, J. C., Hearty, F., Skrutskie, M. F., Majewski, S., Schiavon, R., Eisenstein, D., Gunn, J., Blank, B., Henderson, C., Smee, S., Barkhouser, R., Harding, A., Fitzgerald, G., Stolberg, T., Arns, J., Nelson, M., Brunner, S., Burton, A., Walker, E., Lam, C., Maseman, P., Barr, J., Leger, F., Carey, L., MacDonald, N., Horne, T., Young, E., Rieke, G., Rieke, M., O'Brien, T., Hope, S., Krakula, J., Crane, J., Zhao, B., Carr, M., Harrison, C., Stoll, R., Vernieri, M. A., Holtzman, J., Shetrone, M., Allende-Prieto, C., Johnson, J., Frinchaboy, P., Zasowski, G., Bizyaev, D., Gillespie, B., and Weinberg, D., "The Apache Point Observatory Galactic Evolution Experiment (APOGEE) high-resolution near-infrared multi-object fiber spectrograph," in [*Society of Photo-Optical Instrumentation Engineers (SPIE) Conference Series*], *Society of Photo-Optical Instrumentation Engineers (SPIE) Conference Series* **7735** (July 2010).

[5] Urbach, F., "The long-wavelength edge of photographic sensitivity and of the electronic absorption of solids," *Phys. Rev.* **92**, 1324–1324 (Dec 1953).

[6] Mahadevan, S., Halverson, S., Ramsey, L., and Venditti, N., "Suppression of Fiber Modal Noise Induced Radial Velocity Errors for Bright Emission-line Calibration Sources," *ApJ* **786**, 18 (May 2014).

[7] Halverson, S., Mahadevan, S., Ramsey, L., Hearty, F., Wilson, J., Holtzman, J., Redman, S., Nave, G., Nidever, D., Nelson, M., Venditti, N., Bizyaev, D., and Fleming, S., "Development of Fiber Fabry-Perot Interferometers as Stable Near-infrared Calibration Sources for High Resolution Spectrographs," *Publication of the Astronomical Society of the Pacific* **126**, 445–458 (May 2014).

[8] Redman, S. L., Lawler, J. E., Nave, G., Ramsey, L. W., and Mahadevan, S., "The Infrared Spectrum of Uranium Hollow Cathode Lamps from 850 nm to 4000 nm: Wavenumbers and Line Identifications from Fourier Transform Spectra," *Astrophysical Journals* **195**, 24 (Aug. 2011).

[9] Redman, S. L., Ycas, G. G., Terrien, R., Mahadevan, S., Ramsey, L. W., Bender, C. F., Osterman, S. N., Diddams, S. A., Quinlan, F., Lawler, J. E., and Nave, G., "A High-resolution Atlas of Uranium-Neon in the H Band," *ApJS* **199**, 2 (Mar. 2012).

[10] Cegla, H. M., Shelyag, S., Watson, C. A., and Mathioudakis, M., "Stellar Surface Magneto-convection as a Source of Astrophysical Noise. I. Multi-component Parameterization of Absorption Line Profiles," *Astrophysical Journal* **763**, 95 (Feb. 2013).

[11] Schmidt, S. J., Kowalski, A. F., Hawley, S. L., Hilton, E. J., Wisniewski, J. P., and Tofflemire, B. M., "Probing the Flare Atmospheres of M Dwarfs Using Infrared Emission Lines," *Astrophyscial Journal* **745**, 14 (Jan. 2012).

[12] Robertson, P., Endl, M., Cochran, W. D., and Dodson-Robinson, S. E., "Hα Activity of Old M Dwarfs: Stellar Cycles and Mean Activity Levels for 93 Low-mass Stars in the Solar Neighborhood," *Astrophysical Journal* **764**, 3 (Feb. 2013).

[13] Dumusque, X., Pepe, F., Lovis, C., Ségransan, D., Sahlmann, J., Benz, W., Bouchy, F., Mayor, M., Queloz, D., Santos, N., and Udry, S., "An Earth-mass planet orbiting α Centauri B," *Nature* **491**, 207–211 (Nov. 2012).

[14] Robertson, P., Mahadevan, S., Endl, M., and Roy, A., "Stellar Activity Masquerading as Planets in the Habitable Zone of the M dwarf Gliese 581," *ArXiv e-prints* (July 2014).

[15] Boisse, I., Bonfils, X., and Santos, N. C., "SOAP. A tool for the fast computation of photometry and radial velocity induced by stellar spots," *Astronomy & Astrophysics* **545**, A109 (Sept. 2012).

[16] Udry, S., Bonfils, X., Delfosse, X., Forveille, T., Mayor, M., Perrier, C., Bouchy, F., Lovis, C., Pepe, F., Queloz, D., and Bertaux, J.-L., "The HARPS search for southern extra-solar planets. XI. Super-Earths (5 and 8 M in a 3-planet system," *Astronomy & Astrophysics* **469**, L43–L47 (July 2007).

[17] Mayor, M., Bonfils, X., Forveille, T., Delfosse, X., Udry, S., Bertaux, J.-L., Beust, H., Bouchy, F., Lovis, C., Pepe, F., Perrier, C., Queloz, D., and Santos, N. C., "The HARPS search for southern extra-solar planets. XVIII. An Earth-mass planet in the GJ 581 planetary system," *Astronomy & Astrophysics* **507**, 487–494 (Nov. 2009).

[18] Vogt, S. S., Butler, R. P., Rivera, E. J., Haghighipour, N., Henry, G. W., and Williamson, M. H., "The Lick-Carnegie Exoplanet Survey: A 3.1 M Planet in the Habitable Zone of the Nearby M3V Star Gliese 581," *Astrophysical Journal* **723**, 954–965 (Nov. 2010).

[19] Marchwinski, R. C., Mahadevan, S., Robertson, P., W., R. L., and W., H. J., "Towards Understanding Stellar Radial Velocity Jitter as a Function of Wavelength: The Sun as a Proxy," *(in prep.)* .

[20] Barnes, J. R., Jenkins, J. S., Jones, H. R. A., Jeffers, S. V., Rojo, P., Arriagada, P., Jordán, A., Minniti, D., Tuomi, M., Pinfield, D., and Anglada-Escudé, G., "Precision radial velocities of 15 M5-M9 dwarfs," *Monthly Notices of the Royla Astronomical Society* **439**, 3094–3113 (Apr. 2014).

[21] Kafka, S. and Honeycutt, R. K., "Spectroscopy of Active and Inactive M Dwarfs in Praesepe," *Astronomical Journal* **132**, 1517–1526 (Oct. 2006).

[22] Schlieder, J. E., Lépine, S., Rice, E., Simon, M., Fielding, D., and Tomasino, R., "The Na 8200 Å Doublet as an Age Indicator in Low-mass Stars," *Astronomical Journal* **143**, 114 (May 2012).